Specific Mutations in Transmembrane Helix 8 of Human Concentrative Na + /Nucleoside Cotransporter hCNT1 Affect Permeant Selectivity and Cation Coupling †

ARTICLE *in* BIOCHEMISTRY · MARCH 2007

Impact Factor: 3.02 · DOI: 10.1021/bi061692s · Source: PubMed

Specific Mutations in Transmembrane Helix 8 of Human Concentrative Na^+/Nucleoside Cotransporter hCNT1 Affect Permeant Selectivity and Cation Coupling†

Melissa D. Slugoski,‡,§ Shaun K. Loewen,‡,§ Amy M. L. Ng,‡ Kyla M. Smith,‡ Sylvia Y. M. Yao,‡ Edward Karpinski,‡ Carol E. Cass,|| Stephen A. Baldwin,⊥ and James D. Young*,‡

Membrane Protein Research Group, Departments of Physiology and Oncology, University of Alberta and Cross Cancer Institute, Edmonton, Alberta T6G 2H7, Canada, and Institute of Membrane and Systems Biology, University of Leeds, Leeds LS2 9JT, United Kingdom

Received August 18, 2006; Revised Manuscript Received November 28, 2006

ABSTRACT: The Na^+/nucleoside cotransporters hCNT1 (650 residues) and hCNT2 (658 residues) are 72% identical in amino acid sequence and contain 13 putative transmembrane helices (TMs). Both transport uridine and adenosine but are otherwise selective for pyrimidine (system *cit*) and purine (system *cif*) nucleosides, respectively. Previously, we used site-directed mutagenesis and functional expression in *Xenopus* oocytes to identify two pairs of adjacent residues in TMs 7 and 8 of hCNT1 (Ser^{319}-Gln^{320} and Ser^{353}-Leu^{354}) that, when converted to the corresponding residues in hCNT2 (Gly-Met and Thr-Val, respectively), changed the permeant selectivity of the transporter from *cit* to *cif*. We now report an investigation of the effects of corresponding mutations in TM 8 alone and demonstrate unique S353T- and L354V-induced changes in nucleoside specificity and cation coupling, respectively. hCNT1 mutation S353T produced a profound decrease in cytidine transport efficiency (V_{max}/K_m ratio) and, in combination with L354V (S353T/L354V), resulted in a novel uridine-preferring transport phenotype. In addition, the L354V mutation markedly increased the apparent affinity of hCNT1 for Na^+ and Li^+. Both hCNT1 TM 8 residues exhibited uridine-protectable inhibition by *p*-chloromercuribenzene sulfonate when converted to Cys, suggesting that they occupy positions within or closely adjacent to a common cation/nucleoside translocation pore.

Physiological nucleosides and most therapeutic nucleoside analogues are hydrophilic molecules that require specialized nucleoside transport proteins (NTs)[1] to pass across cellular membranes (*1*−*3*). NT-mediated transport is a critical determinant of intracellular nucleoside metabolism and the pharmacological actions of antineoplastic and antiviral nucleoside drugs (*3*, *4*). By regulating adenosine concentrations in the vicinity of cell surface purinoreceptors, NTs also profoundly affect neurotransmission, vascular tone, and other processes (*5*, *6*). Two structurally unrelated NT protein families exist in mammalian cells: the SLC28 concentrative nucleoside transporter (CNT) family (*7*−*13*) and the SLC29 equilibrative nucleoside transporter (ENT) family (*14*−*17*).

In humans (h), hENT1 and hENT2 mediate facilitated diffusion of nucleosides down their concentration gradients, whereas hCNT1, hCNT2, and hCNT3 couple uphill nucleoside transport to downhill Na^+ transport and, in the case of hCNT3, also downhill transport of H^+. Together, these proteins account for the five major nucleoside transport processes present in human cells. hENT1 and hENT2 are distinguished by different sensitivities (hENT1 > hENT2) to inhibition by nitrobenzylmercaptopurine ribonucleoside (NBMPR) and correspond to functional nucleoside transport systems *es*[2] and *ei*, respectively. Both are broadly selective for pyrimidine and purine nucleosides, while hENT2 also transports nucleobases. ENTs appear to be expressed ubiquitously in mammalian cells. In addition to hENT1 and -2, two other human ENT isoforms have been identified. hENT3

† This work was supported by the National Cancer Institute of Canada with funds from the Canadian Cancer Society, the Alberta Cancer Board, the Heart and Stroke Foundation of Canada, and the Medical Research Council of the United Kingdom. J.D.Y. is a Heritage Scientist of the Alberta Heritage Foundation for Medical Research. C.E.C. is a Canada Research Chair in Oncology at the University of Alberta. M.D.S. and S.K.L. were funded by studentships from the Alberta Heritage Foundation for Medical Research.

* To whom correspondence should be addressed: Department of Physiology, 7-55 Medical Sciences Building, University of Alberta, Edmonton, Alberta T6G 2H7, Canada. Telephone: (780) 492-5895. Fax: (780) 492-7566. E-mail: james.young@ualberta.ca.

‡ Department of Physiology, University of Alberta.

§ These authors contributed equally to this work.

|| Department of Oncology, University of Alberta and Cross Cancer Institute.

⊥ University of Leeds.

[1] Abbreviations: NT, nucleoside transporter; CNT, concentrative nucleoside transporter; ENT, equilibrative nucleoside transporter; NBMPR, nitrobenzylmercaptopurine ribonucleoside {6-[(4-nitrobenzyl)-thio]-9-β-D-ribofuranosylpurine}; TM, putative transmembrane helix; HEPES, 4-(2-hydroxyethyl)-1-piperazineethanesulfonic acid; MES, 2-(*N*-morpholino)ethanesulfonic acid; PCMBS, *p*-chloromercuribenzene sulfonate; MBSS, MES-buffered saline for silica.

[2] Abbreviations used in transporter acronyms: *c*, concentrative; *e*, equilibrative; *s* and *i*, sensitive and insensitive to inhibition by NBMPR, respectively; *f*, formycin B (nonmetabolized purine nucleoside); *t*, thymidine; *b*, broad selectivity.

10.1021/bi061692s CCC: $37.00
Published on Web 01/17/2007

is localized in intracellular membranes and is pH-dependent, while hENT4 is a dual adenosine/monoamine transporter (*18*−*22*). hCNT1 (system *cit*) transports pyrimidine nucleosides and adenosine; hCNT2 (system *cif*) transports purine nucleosides and uridine, and hCNT3 (system *cib*) resembles the broadly selective hENT1 and -2 and transports both pyrimidine and purine nucleosides. In contrast to ENTs, CNTs are found predominantly in intestinal and renal epithelia and other specialized cells, suggesting an important role in absorption, secretion, distribution, and elimination of nucleosides and nucleoside drugs.

While considerable progress has been made in elucidating the structural basis of ENT proteins (*19*), studies of structurally and functionally important residues within the CNT protein family are still at an early stage. hCNT1−3 and other eukaryote CNT family members have a predicted 13-transmembrane helix (TM) architecture, and multiple alignments reveal strong sequence similarities within the carboxyl terminal half of the proteins, particularly within putative TM regions. Previously, we used hCNT1 and -2 sequence comparisons, chimeric constructs, and site-directed mutagenesis in combination with heterologous expression in *Xenopus* oocytes to identify key residues involved in hCNT1 substrate selectivity (*23*). Two pairs of residues in TMs 7 and 8 of hCNT1 (Ser^{319}-Gln^{320} and Ser^{353}-Leu^{354}) were identified that, when converted together to the corresponding residues in hCNT2 (Gly-Met and Thr-Val, respectively), changed the permeant selectivity of the transporter from pyrimidine nucleoside-selective (*cit*) to purine nucleoside-selective (*cif*). Mutation of Ser^{319} in TM 7 of hCNT1 to Gly enabled transport of purine nucleosides, and concurrent mutation of Gln^{320} to Met augmented this transport. The additional mutation of Ser^{353} in TM 8 of hCNT1 to Thr converted S319G/Q320M from broadly selective (*cib* type) to purine nucleoside-selective (*cif* type), but with relatively low adenosine transport activity. Further mutation of Leu^{354} to Val enhanced the adenosine transport capability of S319G/Q320M/S353T, producing a full *cif*-type phenotype. Residues in both TMs 7 and 8 therefore play key roles in determining hCNT1 and -2 nucleoside selectivity.

To further explore the structural and functional significance of hCNT1 TM 8 residues, we report here a follow-up series of experiments in which TM 8 residues Ser^{353} and Leu^{354} were subjected to site-directed mutagenesis in the absence of changes to TM 7. The results reveal dual effects on both nucleoside specificity and cation coupling and, combined with findings from cysteine-directed protein chemistry studies, suggest that the two adjacent TM 8 residues face a common water-accessible cation/nucleoside translocation pathway.

EXPERIMENTAL PROCEDURES

Site-Directed Mutagenesis of hCNT1 and Expression in Xenopus laevis Oocytes. hCNT1 cDNA (GenBank accession number U62968) in *Xenopus* oocyte expression vector pGEM-HE (*24*) provided the template for construction of hCNT1 mutants using the QuikChange mutagenesis kit (Stratagene, La Jolla, CA). By providing 5′- and 3′-untranslated regions from the *Xenopus* β-globin gene flanking the multiple cloning site, pGEM-HE gave greater functional activity than the pBluescript II KS(+) (Stratagene) vector used in earlier studies (*23*). Constructs were sequenced in both directions to confirm that only the correct mutation had been introduced. Plasmid DNA was linearized with *Nhe*I and transcribed with T7 polymerase using the mMESSAGE mMACHINE (Ambion, Austin, TX) transcription system. Defolliculated stage VI *X. laevis* oocytes were microinjected with 20 nL of water or 20 nL of water containing capped RNA transcript (20 ng) and incubated in modified Barth's medium (changed daily) at 18 °C for 72 h prior to the assay of nucleoside transport activity.

Radioisotope Flux Studies. Transport assays were performed as described previously (*13*, *23*) on groups of 10−12 oocytes at room temperature (20 °C) using 1 μCi/mL ^{14}C-labeled or 2 μCi/mL ^{3}H-labeled nucleosides (Moravek Biochemicals, Brea, CA, or Amersham Pharmacia Biotech, Baie d'Urfe, QC) in 200 μL of the appropriate transport medium containing either 100 mM NaCl, 100 mM choline chloride (ChCl), or 100 mM LiCl and 2 mM KCl, 1 mM $CaCl_2$, 1 mM $MgCl_2$, and 10 mM HEPES (pH 7.5) or 10 mM MES (pH 5.5). In cation activation experiments where the indicated Na^+ or Li^+ concentration was less than 100 mM, Na^+ or Li^+ in the transport medium was replaced with equimolar choline$^+$ to maintain isomolarity. Except where otherwise indicated, nucleoside uptake was assessed at a concentration of 20 μM. All uptake values, at both high and low permeant concentrations, represent initial rates of transport (e.g., 7, 9, 10, and 23) determined using an incubation period of 1−10 min, depending upon the construct and coupling cation used in the experiment and have units of picomoles per oocyte per minute. At the end of the incubation period, extracellular radiolabel was removed by seven rapid washes in ice-cold ChCl transport medium (pH 7.5), and individual oocytes were dissolved in 1% (w/v) SDS for quantitation of cell-associated radioactivity by liquid scintillation counting (LS 6000 IC, Beckman, Fullerton, CA). The flux values shown are means ± the standard error (SE) of 10−12 oocytes. Values for the transporter-mediated component of uptake were calculated as uptake in RNA-injected oocytes minus uptake in oocytes injected with water alone. Flux values varied in different batches of oocytes by a maximum of 3-fold between experiments. Kinetic (K_m, K_{50}, V_{max}, and Hill coefficient) parameters (±SE) were calculated from mediated data using ENZFITTER (Elsevier-Biosoft, Cambridge, U.K.).

Electrophysiology Current Measurements. Membrane currents were measured at room temperature (20 °C) using the whole-cell, two-electrode voltage clamp technique (GeneClamp 500B, Axon Instruments Inc., Foster City, CA). The microelectrodes were filled with 3 M KCl and had resistances ranging from 0.5 to 1.5 MΩ. The GeneClamp 500B device was interfaced with a dedicated computer via a Digidata 1322A A/D converter and controlled with Axoscope software (Axon Instruments Inc.). Current signals were filtered at 20 Hz (four-pole Bessel filter) at a sampling interval of 50 ms. For data presentation, the signals were further filtered at 0.75 Hz by using pCLAMP (version 9.0, Axon Instruments Inc.). Following microelectrode penetration, the resting membrane potential was measured over a 15 min period prior to the start of the experiment. Oocytes exhibiting an unstable membrane potential or a potential of less than −30 mV were discarded. Individual oocytes with good resting membrane potentials were clamped at −50 mV, and current measure-

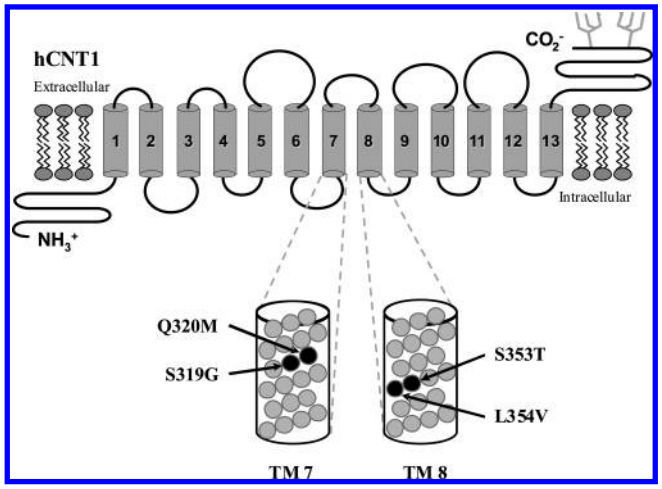

FIGURE 1: hCNT1 topology model. Putative membrane-spanning α-helices are numbered, and glycosylation sites are indicated by the ψ-like symbol in the extracellular C-terminal tail. Residues identified in hCNT1 to be important for substrate selectivity are shown in the expanded TMs 7 and 8 as black circles.

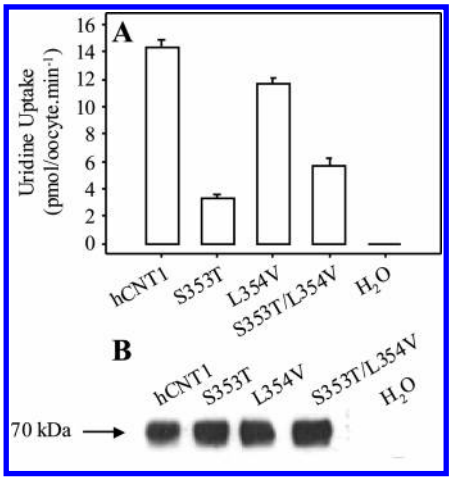

FIGURE 2: Functional activity and protein expression levels of hCNT1-, S353T-, L354V-, and S353T/L354V-producing oocytes. *Xenopus* oocytes injected with RNA transcripts encoding hCNT1, S353T, L354V, or S353T/L354V and control water-injected oocytes were assayed for functional activity by uptake of 20 μM radiolabeled uridine in 100 mM NaCl transport medium (pH 7.5) (A) and plasma membrane recombinant protein expression by Western blotting (B). Flux assay values are the means ± SE from a group of 10−12 oocytes. Flux values that are less than the thickness of the line appear as zero.

ments were obtained in 100 mM NaCl (pH 7.5), ChCl (pH 5.5), or LiCl (pH 7.5) transport media with the same composition used in the radioisotope transport assays. To initiate transport, the medium perfusing the oocyte was changed to one containing 1 mM uridine for approximately 40 s and then exchanged with fresh medium lacking the nucleoside permeant.

PCMBS Inhibition Studies. Oocytes were preincubated on ice for 10 min in 200 μL of 100 mM NaCl transport medium at pH 7.5 containing varying concentrations of *p*-chloromercuribenzene sulfonate (PCMBS) either alone or in the presence of 20 mM nonradioactive uridine, as indicated. The oocytes were then washed three times with ice-cold transport medium and assayed for uridine transport activity (20 μM, 1 min flux).

Western Blots. Purified plasma membranes were prepared from groups of 100 oocytes using silica beads as described by Kamsteeg and Deen (*25*). Protein concentrations were determined by the bicinchoninic acid protein assay (Pierce, Rockford, IL) using BSA as a standard. Aliquots (1 μg) of plasma membrane proteins were resolved on 12% SDS−polyacrylamide gels, and the electrophoresed proteins were transferred to polyvinylidene difluoride membranes and probed with affinity-purified rabbit anti-hCNT1$_{31-55}$ antibodies (*26*). Blots were then incubated with horseradish peroxidase-conjugated anti-rabbit antibodies (Amersham Pharmacia Biotech) and developed with enhanced chemiluminescence reagents (Amersham Pharmacia Biotech).

RESULTS AND DISCUSSION

In humans, hCNT1−3 are functionally distinguished on the basis of substrate selectivity. All three proteins transport uridine and adenosine but are otherwise pyrimidine nucleoside-selective (hCNT1), purine nucleoside-selective (hCNT2), or broadly selective for both pyrimidine and purine nucleosides (hCNT3). Previously, we identified two pairs of isoform-specific residues in the central regions of TMs 7 and 8 of hCNT1 (Ser^{319}-Gln^{320} and Ser^{353}-Leu^{354}, respectively) that, when converted to the corresponding residues in hCNT2 (Gly^{313}-Met^{314} and Thr^{347}-Val^{348}, respectively) (Figure 1), changed the nucleoside specificity of the protein to that of a hCNT2-like transporter (*23*). The goal of this study was to examine the role of the two hCNT1 TM 8 residues (Ser^{353} and Leu^{354}) independent of those in TM 7.

Surface Expression of hCNT1 TM 8 Mutants. Wild-type hCNT1, the two individual hCNT1 mutants, S353T and L354V, and the double hCNT1 mutant, S353T/L354V, all exhibited uptake of radiolabeled uridine (20 μM) in 100 mM NaCl transport medium (pH 7.5) when produced in *Xenopus* oocytes (Figure 2A). In contrast, only basal nonmediated uptake of uridine was evident in control water-injected oocytes under the same conditions. Western blots of purified oocyte plasma membranes revealed similar levels of surface expression for each of the constructs, and wild-type and mutant hCNT1 proteins migrated with an apparent molecular mass of ∼70 kDa (Figure 2B). Antibody specificity for hCNT1 was evident from the lack of immunoreactivity in control water-injected oocytes. Thus, the introduced mutations did not effect cell surface processing of the recombinant proteins.

Nucleoside Specificities of hCNT1 TM 8 Mutants. As an extension of our previous study (*23*) and to assess the effects of TM 8 mutations on permeant selectivity, initial experiments compared wild-type hCNT1 uptake of a panel of radiolabeled pyrimidine and purine nucleosides to that of S353T, L354V, and S353T/L354V (Figure 3). Mediated transport, defined as the difference in uptake between RNA transcript-injected and control water-injected oocytes, was assessed at nucleoside concentrations of 20 μM in 100 mM NaCl transport medium (pH 7.5). The rate of uptake in water-injected oocytes was <0.08 pmol oocyte^{-1} min^{-1} for all nucleosides tested (thymidine > inosine > cytidine > guanosine > uridine > adenosine) (data not shown). In agreement with previous studies (*23*, *30*−*32*), the fluxes in Figure 3A show hCNT1 to be selective for pyrimidine nucleosides (uridine > thymidine > cytidine), with no measurable uptake of inosine and guanosine. Previous studies have established that adenosine is a high-affinity, low-

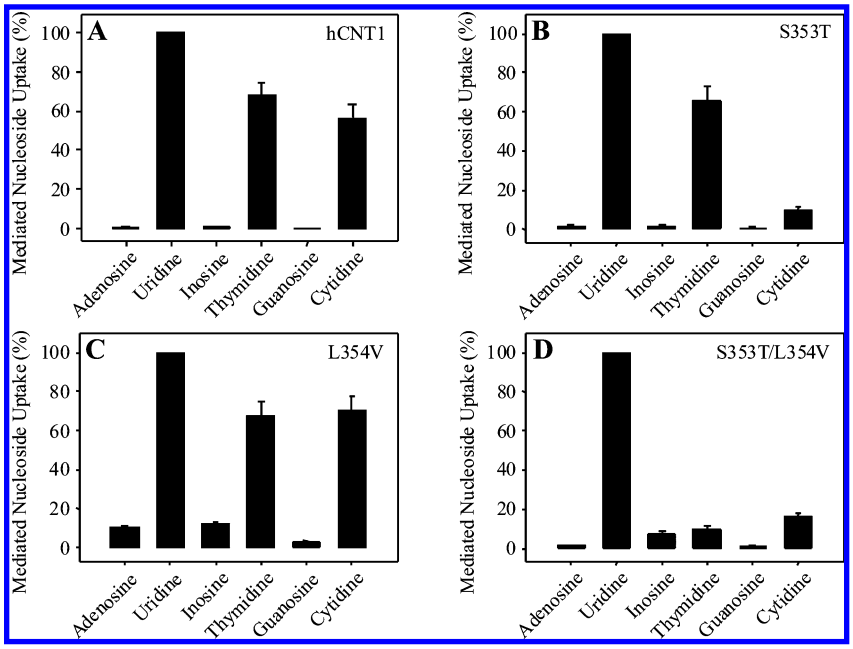

FIGURE 3: Nucleoside selectivity of hCNT1-, S353T-, L354V-, and S353T/L354V-producing oocytes. *Xenopus* oocytes were injected with RNA transcripts encoding hCNT1 (A), S353T (B), L354V (C), or S353T/L354V (D). The rate of uptake of a panel of radiolabeled physiological nucleosides (adenosine, uridine, inosine, thymidine, guanosine, and cytidine) at a concentration of 20 μM was measured in transport medium containing 100 mM NaCl (pH 7.5). Data are presented as mediated transport, calculated as the rate of uptake in RNA-injected oocytes minus the rate of uptake in oocytes injected with water alone, and normalized to the mediated uridine uptake for each transport protein. Mediated uridine fluxes were 6.1 $\pm$ 0.4 (hCNT1), 1.3 $\pm$ 0.1 (S353T), 3.8 $\pm$ 0.3 (L354V), and 2.7 $\pm$ 0.3 pmol oocyte^{-1} min^{-1} (S353T/L354V). Each value represents the mean $\pm$ SE of 10−12 oocytes. Mediated uptake values that are less than the thickness of the line appear as zero. Experiments were performed on the same batch of oocytes used on the same day.

capacity permeant of human and rat CNT1 (*9*, *10*). The apparent lack of adenosine transport shown by hCNT1 in Figure 3A reflects the very low V_{max}/K_m ratio exhibited by this permeant. Like that of hCNT1, pyrimidine nucleoside-selective uptake was evident for both S353T (Figure 3B) and L354V (Figure 3C), although relative to the rate of uridine uptake, the rate of transport of cytidine by S353T was significantly reduced. Additionally, L354V (Figure 3C) exhibited a modestly elevated rate of transport of purine nucleosides (adenosine > inosine > guanosine). This is in good agreement with our previous finding that the L354V mutation augmented adenosine transport by the double TM 7 mutant S319G/Q320M, an effect that occurred through an increase in adenosine V_{max}, with no change in the apparent K_m (*23*). In contrast to the individual mutations, the double mutant S353T/L354V (Figure 3D) exhibited a unique uridine-selective phenotype with only low levels of uptake for other pyrimidine and purine nucleosides (uridine ≫ inosine, thymidine, and cytidine > adenosine and guanosine). Similar to that of L354V, a corresponding small elevation in the rate of inosine transport was also apparent for S353T/L354V (Figure 3D).

Nucleoside Inhibition of Uridine Uptake by hCNT1, S353T, L354V, and S353T/L354V. To determine if mutation-induced changes in hCNT1 permeant selectivity resulted from modifications to the nucleoside binding pocket and/or changes in nucleoside translocation, the rate of uptake of 20 μM radiolabeled uridine [100 mM NaCl (pH 7.5)] by wild-type hCNT1, S353T, L354V, and S353T/L354V was measured in the presence of excess (1 mM) nonradioactive nucleosides (Figure 4). In agreement with the nucleoside uptake profile shown in Figure 3A, uridine uptake by wild-type hCNT1 was inhibited by >91% in the presence of adenosine, uridine, thymidine, and cytidine, with lower levels of inhibition evident for inosine (20%) and guanosine (27%) (Figure 4A). Inhibition profiles similar to that of hCNT1 were seen for S353T (Figure 4B), L354V (Figure 4C), and S353T/L354V (Figure 4D), except that L354V and S353T/L354V exhibited modestly increased levels of inhibition by inosine and guanosine (L354V) and inosine (S353T/L354V), which reflects the slightly elevated rate of uptake of these nucleosides seen in panels C and D of Figure 3, respectively. The marked inhibition of hCNT1-mediated uridine uptake by adenosine (Figure 4A), but apparent lack of adenosine transport in Figure 3A, reflected previous demonstrations of this nucleoside's role as a high-affinity, low-capacity hCNT1 permeant (*9*, *10*) and was shared by all three mutant proteins (Figures 3B−D and 4B−D). Potentially similar behavior was also apparent for cytidine interactions with mutant S353T (Figures 3B and 4B) and for both cytidine and thymidine interactions with mutant S353T/L354V (Figures 3D and 4D). Thus, despite exhibiting altered nucleoside transport profiles, the hCNT1 mutant proteins maintained relatively unaltered nucleoside binding pockets in that they retained thymidine and cytidine binding activities. This was confirmed for the uridine-selective S353T/L354V mutant in the experiments depicted in Figure 5 which examined the concentration dependence of thymidine inhibition of uridine uptake (20 μM). Thymidine effectively inhibited both wild-type hCNT1 and S353T/L354V with broadly similar IC_{50} values of 55 $\pm$ 9 and 26 $\pm$ 4 μM, respectively.

Kinetic Properties of hCNT1 TM 8 Mutants. To further characterize the differences in pyrimidine nucleoside uptake that are evident in Figures 3 and 4, we determined kinetic parameters of the influx of radiolabeled uridine, thymidine, and cytidine in *Xenopus* oocytes producing wild-type hCNT1

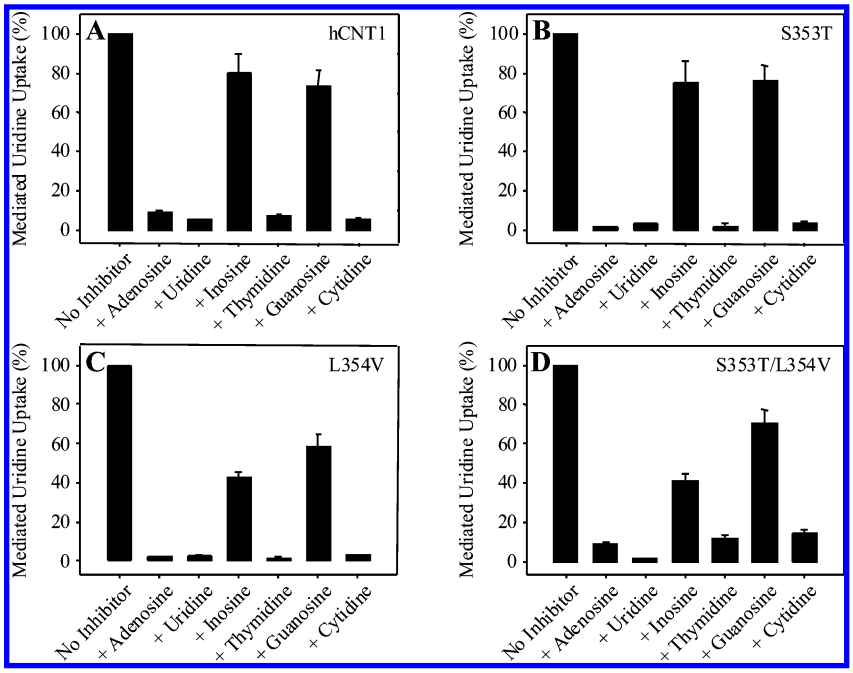

FIGURE 4: Inhibition of hCNT1-, S353T-, L354V-, and S353T/L354V-mediated uridine uptake by physiological nucleosides. hCNT1-mediated (A), S353T-mediated (B), L354V-mediated (C), and S353T/L354V-mediated (D) uptake of 20 μM radiolabeled uridine was assessed in the presence and absence of a panel of physiological nucleosides (adenosine, uridine, inosine, thymidine, guanosine, and cytidine) at a concentration of 1 mM in transport medium containing 100 mM NaCl (pH 7.5). Data are presented as mediated transport, calculated as the rate of uptake in RNA-injected oocytes minus the rate of uptake in oocytes injected with water alone, and normalized to the rate of uptake in the absence of inhibitor for each transport protein. Mediated uridine fluxes were 7.1 ± 0.6 (hCNT1), 1.7 ± 0.2 (S353T), 3.9 ± 0.2 (L354V), and 2.3 ± 0.2 pmol oocyte^{-1} min^{-1} (S353T/L354V). Each value represents the mean ± SE of 10−12 oocytes. Mediated uptake values that are less than the thickness of the line appear as zero. Experiments were performed on the same batch of oocytes used on the same day.

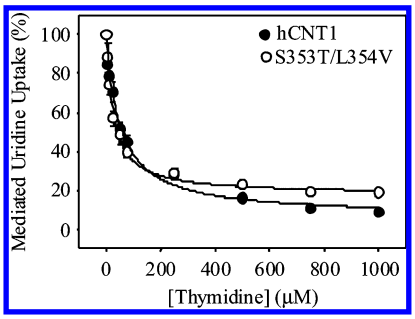

FIGURE 5: Thymidine inhibition of uridine uptake by hCNT1- and S353T/L354V-producing oocytes. The rate of uptake of 20 μM radiolabeled uridine in the presence of increasing concentrations of thymidine was measured in hCNT1-producing (●) and S353T/L354V-producing oocytes (○) in 100 mM NaCl transport medium (pH 7.5). Data are presented as mediated transport, calculated as the rate of uptake in RNA-injected oocytes minus the rate of uptake in water-injected oocytes, and normalized to the mediated uridine uptake rate in the absence of extracellular thymidine. Mediated uridine fluxes in the absence of thymidine were 20 ± 1 (hCNT1) and 8.2 ± 0.5 pmol oocyte^{-1} min^{-1} (S353T/L354V). Each value represents the mean ± SE of 10−12 oocytes. Error bars are not shown in cases where values were smaller than the size of the symbols. Experiments were performed on the same batch of oocytes used on the same day.

and mutants S353T, L354V, and S353T/L354V. Representative concentration dependence curves in 100 mM NaCl transport medium (pH 7.5) for transporter-mediated influx corrected for basal nonmediated uptake measured in control water-injected oocytes are presented in Figure 6. The corresponding kinetic parameters derived from the data are given in Table 1. Control fluxes in water-injected oocytes were linear with respect to nucleoside concentration and <3.0 pmol oocyte^{-1} min^{-1} at 1 mM extracellular nucleoside (thymidine ≫ cytidine > uridine) (data not shown). In all cases, mediated transport was saturable and conformed to simple Michaelis−Menten kinetics. For wild-type hCNT1 (Figure 6A), lower V_{max} values for transport of thymidine and cytidine relative to that of uridine were partly compensated by lower apparent K_m values such that V_{max}/K_m ratios, a measure of transport efficiency, were broadly similar for all three nucleosides (1.24 ± 0.05 for uridine, 0.70 ± 0.06 for thymidine, and 0.57 ± 0.07 for cytidine) (Table 1). Apparent K_m values and the V_{max}/K_m trend of uridine > thymidine > cytidine were consistent with those of previous studies (*23*, *27*−*29*) and are in good agreement with uptake values presented in Figure 3A.

Similarly, results for mutants S353T, L354V, and S353T/L354V (Figure 6B−D) confirmed the findings for uridine, thymidine, and cytidine uptake presented in Figure 3 and established the kinetic basis for the unique uridine-selective phenotype of the S353T/L354V double mutant. Mutant L354V (Figure 6C and Table 1) exhibited an overall decease in both apparent K_m and V_{max} values, and as a result, V_{max}/K_m ratios (1.36 ± 0.12 for uridine, 1.06 ± 0.13 for thymidine, and 0.46 ± 0.03 for cytidine) were similar to those of wild-type hCNT1. In marked contrast, mutant S353T (Figure 6B and Table 1) exhibited substantially reduced V_{max}/K_m ratios (0.35 ± 0.02 for uridine, 0.17 ± 0.02 for thymidine, and 0.02 ± 0.01 for cytidine), with cytidine transport being especially compromised as a consequence of a large decrease in V_{max} (22-fold decrease relative to that of uridine). The combination mutant S353T/L354V (Figure 6D and Table 1) demonstrated efficient transport of uridine similar to that of wild-type hCNT1 (V_{max}/K_m ratios of 1.35 ± 0.10 and 1.24 ± 0.05, respectively) but was severely compromised with

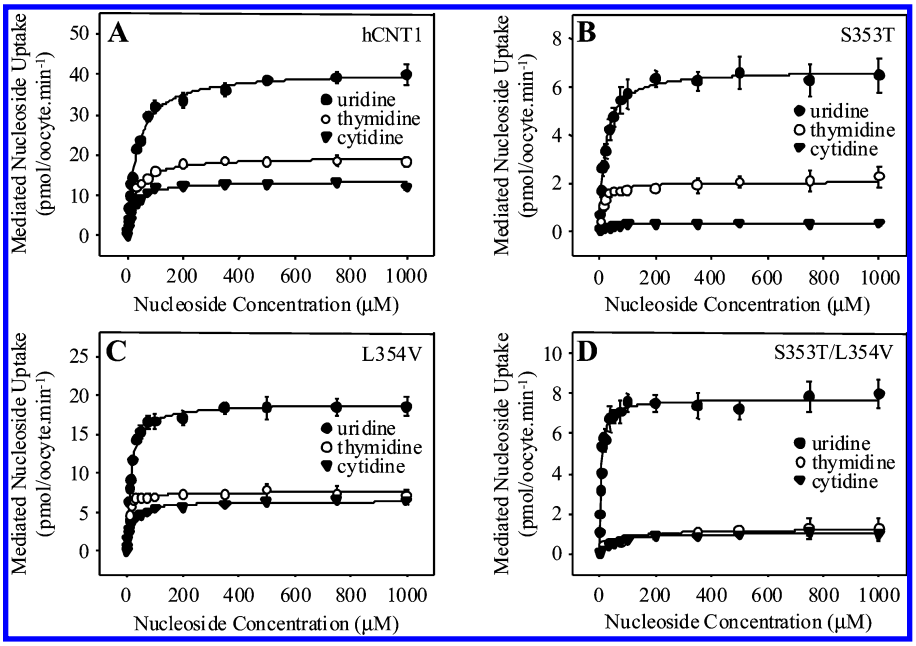

FIGURE 6: Uridine, thymidine, and cytidine uptake kinetics in oocytes producing hCNT1, S353T, L354V, and S353T/L354V. Rates of uptake of radiolabeled uridine (●), thymidine (○), and cytidine (▼) in 100 mM NaCl transport medium (pH 7.5) were measured in hCNT1-producing (A), S353T-producing (B), L354V-producing (C), or S353T/L354V-producing (D) *Xenopus* oocytes. Data are presented as mediated transport, calculated as the rate of uptake in RNA-injected oocytes minus the rate of uptake in oocytes injected with water alone. Each value represents the mean ± SE of 10−12 oocytes. Error bars are not shown in cases where values were smaller than the size of the symbols. Experiments were performed on the same batch of oocytes used on the same day.

Table 1: Kinetic Parameters for Uptake of Uridine, Thymidine, and Cytidine by hCNT1 and hCNT1 Mutants Produced in *Xenopus* Oocytes[a]

transporter	nucleoside	apparent K_m (μM)	V_{max} (pmol oocyte^{-1} min^{-1})	V_{max}/K_m ratio
hCNT1	uridine	33 ± 2	41 ± 1	1.24 ± 0.05
	thymidine	27 ± 2	19 ± 1	0.70 ± 0.06
	cytidine	23 ± 2	13 ± 1	0.57 ± 0.07
S353T	uridine	19 ± 1	6.7 ± 0.1	0.35 ± 0.02
	thymidine	12 ± 1	2.0 ± 0.1	0.17 ± 0.02
	cytidine	16 ± 2	0.3 ± 0.1	0.02 ± 0.01
L354V	uridine	14 ± 1	19 ± 1	1.36 ± 0.12
	thymidine	7.2 ± 0.9	7.6 ± 0.2	1.06 ± 0.13
	cytidine	14 ± 1	6.4 ± 0.1	0.46 ± 0.03
S353T/L354V	uridine	5.7 ± 0.4	7.7 ± 0.1	1.35 ± 0.10
	thymidine	46 ± 9	1.2 ± 0.1	0.03 ± 0.01
	cytidine	41 ± 3	1.1 ± 0.1	0.03 ± 0.01

[a] Values (±SE) taken from Figure 6.

respect to transport of both thymidine and cytidine. As was the case with S353T, low V_{max}/K_m ratios of 0.03 ± 0.01 for transport of thymidine and cytidine by S353T/L354V were the result of large decreases in V_{max} with only moderately increased thymidine and cytidine K_m values in comparison to that of wild-type hCNT1. Overall, the kinetic data confirmed that mutations S353T and S353T/L354V primarily altered pyrimidine nucleoside translocation rather than binding affinities.

Additional Mutants. To investigate the relationship between side chain structure and function, the role of hCNT1 TM 8 residue positions 353 and 354 in determining nucleoside selectivity was further studied through additional mutations by changing Ser^{353} to Ala, Cys, and Val and Leu^{354} to Ala, Cys, Ile, and Met. Mutant proteins were produced in oocytes and assayed for uridine, thymidine, cytidine, and inosine uptake under the same conditions used in Figure 3. Conversion of Ser^{353} of hCNT1 to Ala (S353A), Cys (S353C), or Val (S353V) resulted in proteins with hCNT1-like nucleoside uptake phenotypes, with only basal levels of inosine uptake (<0.1 pmol oocyte^{-1} min^{-1}) and rates of transport in the following order: uridine > thymidine > cytidine (data not shown). Therefore, hydrogen bonding at hCNT1 residue position 353 was not critical for maintaining the pyrimidine nucleoside selectivity of the transporter. Conversion of Leu^{354} to Ala (L354A), Cys (L354C), Ile (L354I), or Met (L354M) also resulted in proteins with hCNT1-like substrate selectivity profiles, with none of the amino acid substitutions mimicking the small L354V increase in the rate of inosine uptake (data not shown).

Cation Specificity of hCNT1 TM 8 Mutants. Mammalian CNTs function predominantly as Na^+-coupled nucleoside transporters. For hCNT3, H^+ and Li^+ have been shown to substitute for Na^+ (*12*, *13*, *30*), a phenomenon also observed with other Na^+-coupled membrane cotransport proteins, including the bacterial MelB melibiose transporter and the mammalian SGLT Na^+-glucose and SDCT1/NaDC-1 Na^+/dicarboxylate cotransporters (*31*−*35*). To investigate whether changes in nucleoside specificity of hCNT1 TM 8 mutants were accompanied by corresponding alterations in cation selectivities, wild-type hCNT1 and mutant S353T, L354V, and S353T/L354V proteins were assayed for radiolabeled uridine uptake (20 μM) in the presence of Na^+ [100 mM NaCl (pH 7.5)], H^+ [100 mM ChCl (pH 5.5)], and Li^+ [100 mM LiCl (pH 7.5)] and in the absence of cation [100 mM ChCl (pH 7.5)] (data not shown). As in previous studies (*27*, *36*), Na^+ was confirmed to be the primary hCNT1 coupling cation with robust uridine uptake in the presence of Na^+ (7.2 ± 0.7 pmol oocyte^{-1} min^{-1}) and only basal levels of uridine uptake in Na^+-free H^+-containing or cation-free medium. Very weak, but significant, hCNT1-mediated uptake of

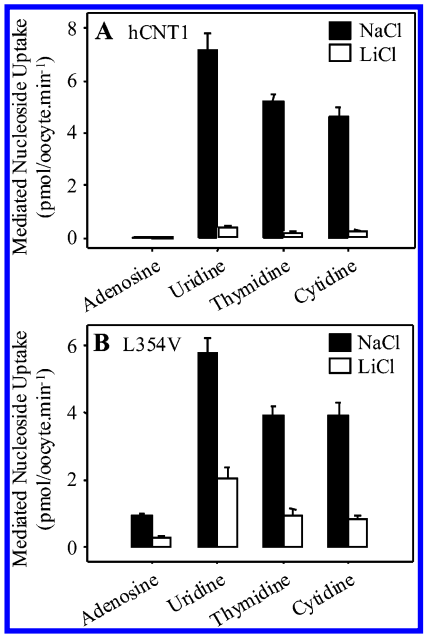

FIGURE 7: Na^+- and Li^+-dependent nucleoside transport by hCNT1 and L354V. The rate of uptake of 20 μM radiolabeled physiological nucleosides (adenosine, uridine, thymidine, and cytidine) in oocytes producing hCNT1 (A) or L354V (B) was measured in transport medium containing 100 mM NaCl (black bars) or LiCl (white bars) (pH 7.5). Data are presented as mediated transport, calculated as the rate of uptake in RNA-injected oocytes minus the rate of uptake in water-injected oocytes. Each value represents the mean ± SE of 10−12 oocytes. Mediated uptake values that are less than the thickness of the line appear as zero. Experiments were performed on the same batch of oocytes used on the same day.

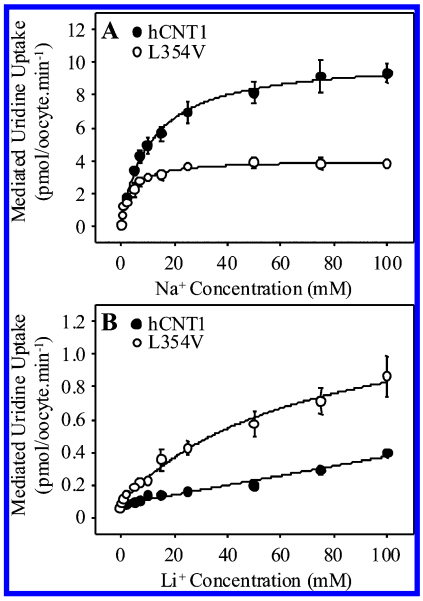

FIGURE 8: hCNT1 and L354V Na^+ and Li^+ activation kinetics. The rate of uptake of 20 μM radiolabeled uridine by hCNT1 (●) and L354V (○) was measured as a function of Na^+ (A) and Li^+ concentration (B), using choline$^+$ as an isosmotic Na^+ substitute (pH 7.5). Data are presented as mediated transport, calculated as the rate of uptake in RNA-injected oocytes minus the rate of uptake in water-injected oocytes. Each value represents the mean ± SE of 10−12 oocytes. Error bars are not shown in cases where values were smaller than the size of the symbols. Experiments were performed on the same batch of oocytes used on the same day.

uridine was seen in Na^+-free Li^+-containing medium (0.16 ± 0.03 pmol oocyte^{-1} min^{-1}). A similar cation selectivity profile was seen for S353T. In contrast, L354V, and to a lesser extent S353T/L354V, exhibited elevated Li^+-mediated uridine transport activity [1.2 ± 0.1 (Li^+) and 5.3 ± 0.4 (Na^+) pmol oocyte^{-1} min^{-1} for L354V and 0.6 ± 0.1 (Li^+) and 3.8 ± 0.1 (Na^+) pmol oocyte^{-1} min^{-1} for S353T/L354V]. Similar to hCNT1, however, L354V and S353T/L354V exhibited only a basal level of uridine uptake in Na^+-free H^+-containing or cation-free medium. L354V Li^+ dependence was most marked for uridine but was also apparent for other nucleosides (adenosine, thymidine, and cytidine) (Figure 7). All of the other residue mutations that were constructed (S353A, S353C, S353V, L354A, L354C, L354I, and L354M) maintained hCNT1-like cation selectivity and were not able to mimic the L354V increase in the rate of Li^+-dependent uridine uptake (data not shown).

Kinetics of Li^+-Dependent Uridine Transport by L354V. Figure 8 compares Na^+ and Li^+ activation curves for wild-type hCNT1 and L354V [20 μM radiolabeled uridine (pH 7.5)]. Both L354V cation activation curves indicated that the Li^+ dependence of L354V reflects a generalized increase in the apparent affinities of the mutant transporter for both Na^+ and Li^+. Apparent K_{50} values for Na^+ activation of hCNT1 and L354V were 12 ± 1 and 3.8 ± 0.4 mM, respectively (Figure 8A), compared to >100 and 71 ± 17 mM, respectively, for Li^+ (Figure 8B). As expected from previous studies (*9*, *10*, *29*, *36*), Hill coefficients for Na^+ activation of hCNT1 and L354V (0.99 ± 0.04 and 0.91 ± 0.08, respectively) were consistent with Na^+:nucleoside coupling stoichiometries of 1:1. Similarly, the Hill coefficient for Li^+ activation of L354V (0.61 ± 0.05) was also consistent with a 1:1 coupling ratio. A Hill coefficient for Li^+-mediated transport by hCNT1 could not be determined because of the low apparent affinity of the wild-type transporter for Li^+.

Previously, we have established that hCNT1 mediates Na^+-coupled nucleoside transport by a sequential ordered binding mechanism in which cation binds to the transporter first, increasing its affinity for the nucleoside, which then binds second (*27*). It was predicted, therefore, that the low apparent affinity of hCNT1 for Li^+ would be matched by a correspondingly low apparent affinity for Li^+-mediated uridine influx and that the Li^+ K_{50} difference between L354V and hCNT1 would be mirrored by a corresponding downward shift in the nucleoside apparent K_m value. The experiments depicted in Figure 9, which confirmed these predictions, compared the concentration dependence of hCNT1- and L354V-mediated radiolabeled uridine influx in Na^+- and Li^+-containing transport medium [100 mM NaCl and LiCl (pH 7.5)]. In agreement with panels A and C of Figure 6 and Table 1, the apparent K_m values for Na^+-mediated uridine transport were 24 ± 2 (hCNT1) and 15 ± 2 μM (L354V). Li^+-mediated uridine uptake was nonsaturable for hCNT1 (Figure 9A) but exhibited an apparent K_m value of 210 ± 20 μM for L354V (Figure 9B). No such K_m shift was apparent for Na^+-mediated uridine uptake (Figure 6A,C and Table 1), because these transport assays were performed at a Na^+ concentration of 100 mM which was sufficient to fully saturate both the mutant and wild-type transporters. The V_{max} value for Li^+-mediated uridine uptake by L354V was similar to that in the presence of Na^+ (9.9 ± 0.3 and 10 ± 1 pmol oocyte^{-1} min^{-1}, respectively).

The electrogenic nature of the Li^+-dependent uridine transport by wild-type hCNT1 and L354V is demonstrated

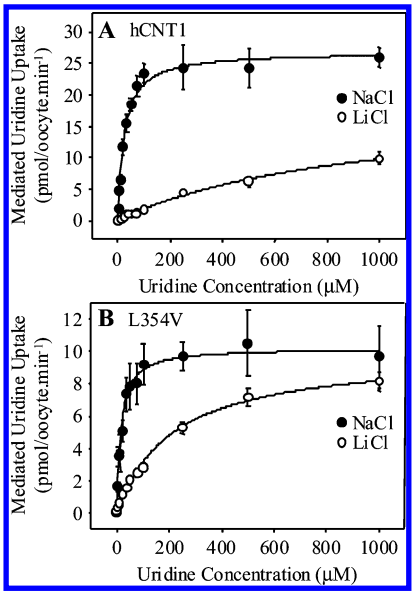

FIGURE 9: Concentration dependence of Na^+- and Li^+-dependent uridine uptake by hCNT1 and L354V. Radiolabeled uridine uptake rates in Na^+-containing (●) and Li^+-containing transport medium (○) were determined in oocytes expressing hCNT1 (A) and L354V (B) [100 mM NaCl or LiCl (pH 7.5)]. Data are presented as mediated transport, calculated as the rate of uptake in RNA-injected oocytes minus the rate of uptake in water-injected oocytes. Each value represents the mean ± SE of 10−12 oocytes. Error bars are not shown in cases where values were smaller than the size of the symbols. Experiments were performed on the same batch of oocytes used on the same day.

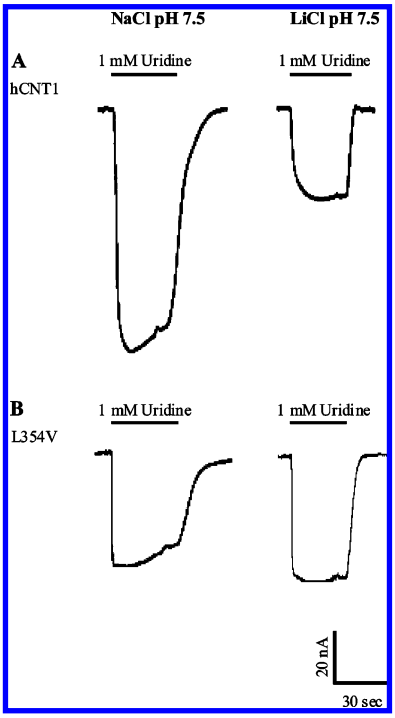

FIGURE 10: Uridine-evoked currents in hCNT1- and L354V-producing oocytes. Uridine-evoked currents in 100 mM NaCl and LiCl transport medium at pH 7.5 (right and left columns, respectively) are shown for representative oocytes producing hCNT1 (A) or L354V (B). No current was detected in control water-injected oocytes (data not shown). Bars indicate the duration of exposure to 1 mM uridine. Currents were recorded in the same batch of oocytes used on the same day.

in Figure 10, which shows results of experiments that used the two-electrode, voltage clamp method to compare representative whole-cell currents induced by 1 mM uridine measured in medium containing either Na^+ [100 mM NaCl (pH 7.5)] or Li^+ [100 mM LiCl (pH 7.5)]. Since the Leu^{354} mutation affected Na^+ and hence uridine apparent binding affinity, the transport difference between L354V and hCNT1 in Li^+ medium was minimized at the high uridine concentration used in this experiment. Thus, the electrophysiology recordings demonstrated uridine-induced Li^+ currents for both L354V and hCNT1. These representative electrophysiology current recordings are consistent with the radioisotope flux data shown in Figure 9.

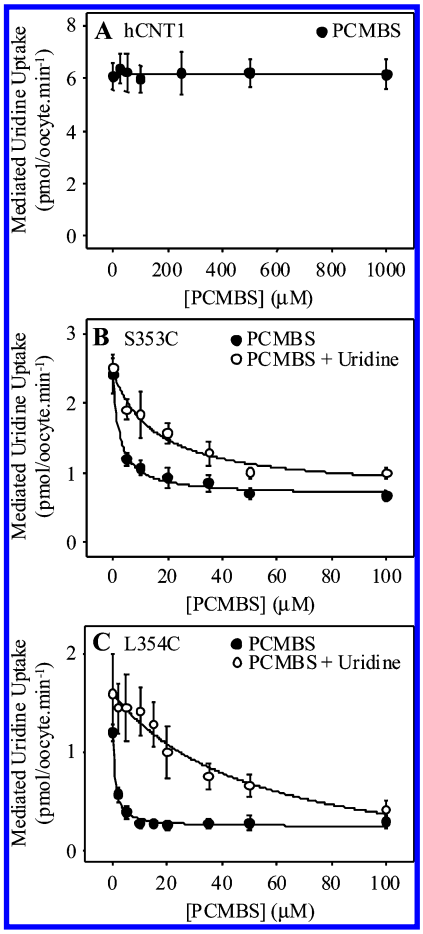

FIGURE 11: PCMBS inhibition of hCNT1-, S353C-, and L354C-mediated uridine transport. Radiolabeled uridine uptake rates (20 μM) were measured in oocytes producing hCNT1 (A), S353C (B), or L354C (C) that had been preincubated in the presence of PCMBS (●) or in the presence of PCMBS and 20 mM uridine (○) [100 mM NaCl (pH 7.5)]. Data are presented as mediated transport, calculated as the rate of uptake in RNA-injected oocytes minus the rate of uptake in water-injected oocytes. Each value represents the mean ± SE of 10−12 oocytes. Error bars are not shown in cases where values were smaller than the size of the symbols. Experiments were performed on the same batch of oocytes used on the same day.

PCMBS Inhibition of S353C- and L354C-Mediated Uridine Transport. Residues lining the translocation pore can be identified through the use of water-soluble thiol-reactive reagents such as membrane-impermeant *p*-chloromercuribenzene sulfonate (PCMBS) (*37*). Although wild-type hCNT1 contains 20 endogenous Cys residues, there was no change in the hCNT1-mediated uptake of 20 μM radiolabeled uridine [100 mM NaCl (pH 7.5)] following preincubation with PCMBS at concentrations up to 1 mM (Figure 11A). However, uridine uptake by both S353C and L354C was

strongly inhibited by low micromolar concentrations of PCMBS, and the presence of extracellular uridine (20 mM) significantly protected both mutants against this inhibition (Figure 11B,C). While previous helix modeling of hCNT1 TM 8 predicted that Ser^{353} faces the translocation pore and Leu^{354} is involved in helix−helix interactions (*23*), the results presented here suggest that both residues are accessible from the extracellular medium, pore-lining, and in the proximity of the uridine-binding pocket. Additional evidence supporting this conclusion is found in a cysteine-free version of hCNT3 in which the corresponding residues, when individually mutated to cysteine, also show inhibition of uridine uptake by PCMBS (unpublished observations).

Conclusions. Mutational analysis of hCNT1 TM 8 Ser^{353} and Leu^{354} has revealed a dual role for these adjacent residues in both nucleoside selectivity and cation coupling. Mutation of these residues to the corresponding residues in hCNT2 resulted in (i) a decreased rate of cytidine transport (S353T), (ii) a unique uridine-selective phenotype (S353T/L354V), (iii) a modest increase in the rate of inosine transport (L354V), and (iv) increased apparent affinities for Na^+ and Li^+ (L354V). In all cases, the alterations in the hCNT1 functional phenotype were amino acid-specific. A possible role for Ser^{353} in forming hydrogen bonds with the nucleoside permeant was discounted by substitution of other amino acids at this position. Competition studies revealed that the S353T/L354V double mutant retained an apparently normal nucleoside binding pocket, its novel uridine-selective transport phenotype resulting instead from changes in the subsequent nucleoside translocation phase of the transport cycle. These results also revealed that wild-type hCNT1 exhibited a low, but significant, affinity for Li^+ as the coupling cation, an interaction that was markedly enhanced in mutant L354V and, to a lesser extent, in S353T/L354V. This is similar to the case for hCNT3, which can utilize Na^+ and Li^+ (and H^+) electrochemical gradients to drive transport (*30*). The L354V and S353T/L354V mutations did not lead to H^+ dependence, indicating different structural requirements for CNT H^+ and Na^+/Li^+ coupling. Mutation of both TM 8 residues to Cys resulted in uridine-protected inhibition by PCMBS. Structurally, this places each of these residues in an orientation facing the translocation pore and in the vicinity of the uridine-binding pocket. This proposed topology, as well as the influence of both hCNT1 TM 8 residues Ser^{353} and Leu^{354}, either alone or in combination, on substrate and cation interactions, therefore suggests closely adjacent interactions of nucleosides and cations within a common hCNT1 translocation pore. The recently reported crystal structure of *Aquifex aeolicus* Leu_{Aa}, a homologue of mammalian Na^+/Cl^--dependent neurotransmitter transporters, depicts a similar structural model for transport in which bound leucine and Na^+ ions are located in close association within the protein core halfway across the membrane with both binding sites being defined by partially unwound transmembrane helices (*38*).

REFERENCES

1. Cass, C. E. (1995) Nucleoside transport, in *Drug Transport in Antimicrobial and Anticancer Chemotherapy* (Georgopapadakou, N. H., Ed.) pp 403−451, Marcel Deker, New York.
2. Griffith, D. A., and Jarvis, S. M. (1996) Nucleoside and nucleobase transport systems of mammalian cells, *Biochim. Biophys. Acta 1286*, 153−181.
3. Cheeseman, C. I., Mackey, J. R., Cass, C. E., Baldwin, S. A., and Young, J. D. (2000) Molecular mechanisms of nucleoside and nucleoside drug transport, in *A Volume of Current Topics in Membranes*, pp 330−379, Academic Press, San Diego.
4. Mackey, J. R., Baldwin, S. A., Young, J. D., and Cass, C. E. (1998) Nucleoside transport and its significance for anticancer drug resistance, *Drug Resist. Updates 1*, 310−324.
5. Dunwiddie, T. V., and Masino, S. A. (2001) The role and regulation of adenosine in the central nervous system, *Annu. Rev. Neurosci. 24*, 31−55.
6. King, A. E., Ackley, M. A., Cass, C. E., Young, J. D., and Baldwin, S. A. (2006) Nucleoside transporters: From scavengers to novel therapeutic targets, *Trends Pharmacol. Sci. 27*, 416−425.
7. Huang, Q. Q., Yao, S. Y. M., Ritzel, M. W. L., Paterson, A. R. P., Cass, C. E., and Young, J. D. (1994) Cloning and functional expression of a complementary DNA encoding a mammalian nucleoside transport protein, *J. Biol. Chem. 269*, 17757−17760.
8. Che, M., Ortiz, D. F., and Arias, I. M. (1995) Primary structure and functional expression of a cDNA encoding the bile canalicular, purine-specific Na^+-nucleoside cotransporter, *J. Biol. Chem. 270*, 13596−13599.
9. Yao, S. Y. M., Ng, A. M. L., Ritzel, M. W. L., Gati, W. P., Cass, C. E., and Young, J. D. (1996) Transport of adenosine by recombinant purine- and pyrimidine-selective sodium/nucleoside cotransporters from rat jejunum expressed in *Xenopus laevis* oocytes, *Mol. Pharmacol. 50*, 1529−1535.
10. Ritzel, M. W. L., Yao, S. Y. M., Huang, M. Y., Elliot, J. F., Cass, C. E., and Young, J. D. (1997) Molecular cloning and functional expression of cDNAs encoding a human Na^+-nucleoside cotransporter (hCNT1), *Am. J. Physiol. 272*, C707−C714.
11. Wang, J., Su, S. F., Dresser, M. J., Schaner, M. E., Washington, C. B., and Giacomini, K. M. (1997) Na^+-dependent purine nucleoside transporter from human kidney: Cloning and functional characterization, *Am. J. Physiol. 273*, F1058−F1065.
12. Ritzel, M. W. L., Yao, S. Y. M., Ng, A. M. L., Mackey, J. R., Cass, C. E., and Young, J. D. (1998) Molecular cloning, functional expression and chromosomal localization of a cDNA encoding a human Na^+/nucleoside cotransporter (hCNT2) selective for purine nucleosides and uridine, *Mol. Membr. Biol. 15*, 203−211.
13. Ritzel, M. W. L., Ng, A. M. L., Yao, S. Y. M., Graham, K., Loewen, S. K., Smith, K. M., Ritzel, R. G., Mowles, D. A., Carpenter, P., Chen, X.-Z., Karpinski, E., Hyde, R. J., Baldwin, S. A., Cass, C. E., and Young, J. D. (2001) Molecular identification and characterization of novel human and mouse concentrative Na^+-nucleoside cotransporter proteins (hCNT3 and mCNT3) broadly selective for purine and pyrimidine nucleosides (system cib), *J. Biol. Chem. 276*, 2914−2927.
14. Griffiths, M., Beaumont, N., Yao, S. Y. M., Sundaram, M., Bouman, C. E., Davies, A., Kwong, F. Y. P., Coe, I. R., Cass, C. E., Young, J. D., and Baldwin, S. A. (1997) Cloning of a human nucleoside transporter implicated in the cellular uptake of adenosine and chemotherapeutic drugs, *Nat. Med. 3*, 89−93.
15. Griffiths, M., Yao, S. Y. M., Abidi, F., Phillips, S. E. V., Cass, C. E., Young, J. D., and Baldwin, S. A. (1997) Molecular cloning and characterization of a nitrobenzylthioinosine-insensitive (ei) equilibrative nucleoside transporter from human placenta, *Biochem. J. 328*, 739−743.
16. Yao, S. Y. M., Ng, A. M. L., Muzyka, W. R., Griffiths, M., Cass, C. E., Baldwin, S. A., and Young, J. D. (1997) Molecular cloning and functional characterization of nitrobenzylthioinosine (NBMPR)-sensitive (es) and NBMPR-insensitive (ei) equilibrative nucleoside transporter proteins (rENT1 and rENT2) from rat tissues, *J. Biol. Chem. 272*, 28423−28430.
17. Crawford, C. R., Patel, D. H., Naeve, C., and Belt, J. A. (1998) Cloning of the human equilibrative, nitrobenzylmercaptopurine riboside (NBMPR)-insensitive nucleoside transporter ei by functional expression in a transport-deficient cell line, *J. Biol. Chem. 273*, 5288−5293.
18. Acimovic, Y., and Coe, I. R. (2002) Molecular evolution of the equilibrative nucleoside transporter family: Identification of novel family members in prokaryotes and eukaryotes, *Mol. Biol. Evol. 19*, 2199−2210.
19. Baldwin, S. A., Beal, P. R., Yao, S. Y. M., King, A. E., Cass, C. E., and Young, J. D. (2004) The equilibrative nucleoside transporter family, SLC29, *Pfluegers Arch. 447*, 735−743.
20. Baldwin, S. A., Yao, S. Y. M., Hyde, R. J., Ng, A. M. L., Foppolo, S., Barnes, K., Ritzel, M. W. L., Cass, C. E., and Young, J. D. (2005) Functional characterization of novel human and mouse

equilibrative nucleoside transporters (hENT3 and mENT3) located in intracellular membranes, *J. Biol. Chem. 280*, 15880−15887.
21. Engel, K., and Wang, J. (2005) Interaction of organic cations with a newly identified plasma membrane monoamine transporter, *Mol. Pharmacol. 68*, 1397−1407.
22. Barnes, K., Dobrzynski, H., Foppolo, S., Beal, P. R., Ismat, F., Scullion, E. R., Sun, L., Tellez, J., Ritzel, M. W. L., Claycomb, W. C., Cass, C. E., Young, J. D., Billeter-Clark, R., Boyett, M. R., and Baldwin, S. A. (2006) Distribution and functional characterization of equilibrative nucleoside transporter-4, a novel cardiac adenosine transporter activated at acidic pH, *Circ. Res.* (in press).
23. Loewen, S. K., Ng, A. M., Yao, S. Y., Cass, C. E., Baldwin, S. A., and Young, J. D. (1999) Identification of amino acid residues responsible for the pyrimidine and purine nucleoside specificities of human concentrative Na^+ nucleoside cotransporters hCNT1 and hCNT2, *J. Biol. Chem. 274*, 24475−24484.
24. Liman, E. R., Tytgat, J., and Hess, P. (1992) Subunit stoichiometry of a mammalian K^+ channel determined by construction of multimeric cDNAs, *Neuron 9*, 861−871.
25. Kamsteeg, E.-J., and Deen, P. M. (2001) Detection of aquaporin-2 in the plasma membranes of oocytes: A novel isolation method with improved yield and purity, *Biochem. Biophys. Res. Commun. 282*, 683−690.
26. Laemmli, U. K. (1970) Cleavage of structural proteins during the assembly of the head of bacteriophage T4, *Nature 277*, 680−685.
27. Smith, K. M., Ng, A. M. L., Yao, S. Y. M., Labedz, K. A., Knaus, E. E., Wiebe, L. I., Cass, C. E., Baldwin, S. A., Chen, X.-Z., Karpinski, E., and Young, J. D. (2004) Electrophysiological characterization of a recombinant human Na^+-coupled nucleoside transporter (hCNT1) produced in *Xenopus* oocytes, *J. Physiol. 558*, 807−823.
28. Lostao, M. P., Mata, J. F., Larrayoz, I. M., Inzillo, S. M., Casado, F. J., and Pastor-Anglada, M. (2000) Electrogenic uptake of nucleosides and nucleoside-derived drugs by the human nucleoside transporter 1 (hCNT1) expressed in *Xenopus laevis* oocytes, *FEBS Lett. 481*, 137−140.
29. Dresser, M. J., Gerstin, K. M., Gray, A. T., Loo, D. D. F., and Giacomini, K. M. (2000) Electrophysiological analysis of the substrate selectivity of a sodium-coupled nucleoside transporter (rCNT1) expressed in *Xenopus laevis* oocytes, *Drug Metab. Dispos. 28*, 1135−1140.
30. Smith, K. M., Slugoski, M. D., Loewen, S. K., Ng, A. M. L., Yao, S. Y. M., Chen, X.-Z., Karpinski, E., Cass, C. E., Baldwin, S. A., and Young, J. D. (2005) The broadly selective human Na^+/nucleoside cotransporter (hCNT3) exhibits novel cation-coupled nucleoside transport characteristics, *J. Biol. Chem. 280*, 25436−25449.
31. Pourcher, T., Bassilana, M., Sarkar, H. K., Kaback, R., and Leblanc, G. (1990) The melibiose/Na^+ symporter of *Escherichia coli*: Kinetic and molecular properties, *Philos. Trans. R. Soc. London, Ser. B 326*, 411−423.
32. Hirayama, B. A., Loo, D. D. F., and Wright, E. M. (1994) Protons drive sugar transport through the Na^+/glucose cotransporter (SGLT1), *J. Biol. Chem. 269*, 21407−21410.
33. Hirayama, B. A., Loo, D. D. F., and Wright, E. M. (1997) Cation effects on protein conformation and transport in the Na^+/glucose cotransporter, *J. Biol. Chem. 272*, 2110−2115.
34. Pajor, A. M., Hirayama, B. A., and Loo, D. D. F. (1998) Sodium and lithium interactions with the Na^+/dicarboxylate cotransporter, *J. Biol. Chem. 273*, 18923−18929.
35. Chen, X.-Z., Shayakul, C., Berger, U. V., Tian, W., and Hediager, M. A. (1998) Characterization of a rat Na^+-dicarboxylate cotransporter, *J. Biol. Chem. 273*, 20972−20981.
36. Smith, K. M., Slugoski, M. D., Cass, C. E., Baldwin, S. A., Karpinski, E., and Young, J. D. (2006) Cation coupling properties of human concentrative nucleoside transporters hCNT1, hCNT2 and hCNT3, *Mol. Membr. Biol.* (in press).
37. Yao, S. Y. M., Sundaram, M., Chomey, E. G., Cass, C. E., Baldwin, S. A., and Young, J. D. (2001) Identification of Cys140 in helix 4 as an exofacial cysteine residue within the substrate-translocation channel of rat equilibrative nitrobenzylthioinosine (NBMPR)-insensitive nucleoside transporter rENT2, *Biochem. J. 353*, 387−393.
38. Yamashita, A., Singh, S. K., Kawate, T., Jin, Y., and Gouaux, E. (2005) Crystal structure of a bacterial homologue of Na^+/Cl^--dependent neurotransmitter transporters, *Nature 437*, 215−223.

BI061692S